Half-metallic graphene nanodots: A comprehensive first-principles theoretical study

Oded Hod,[1] Verónica Barone,[2] and Gustavo E. Scuseria[1]
[1]*Department of Chemistry, Rice University, Houston, Texas 77005-1892, USA*
[2]*Department of Physics, Central Michigan University, Mt. Pleasant, Michigan 48859, USA*
(Received 23 September 2007; published 10 January 2008)

A comprehensive *first-principles* theoretical study of the electronic properties and half-metallic nature of finite rectangular graphene nanoribbons is presented. We identify the bisanthrene isomer of the $C_{28}H_{14}$ molecule to be the smallest graphene derivative to present a spin-polarized ground state. Even at this quantum dot level, the spins are predicted to be aligned antiferromagnetically at the two zigzag edges of the system. As a rule of thumb, we find that zigzag graphene edges that are at least three consecutive units long will present spin polarization if the width of the system is 1 nm or wider. Room temperature detectability of the magnetic ordering is predicted for ribbons with zigzag edges 1 nm and longer. For the longer systems studied, spin wave structures appear in some high spin multiplicity states. Energy gap oscillations with the length of the zigzag edge are observed. The amplitude of these oscillations is found to be smaller than that predicted for infinite ribbons. The half-metallic nature of the ribbons under an external in-plane electric field is found to be preserved even for finite and extremely short systems.

DOI: 10.1103/PhysRevB.77.035411 PACS number(s): 73.22.−f, 85.75.−d, 73.21.La, 75.75.+a

I. INTRODUCTION

Since their recent successful fabrication,[1] graphene nanoribbons (GNRs) have been the focus of extensive experimental and theoretical efforts. GNRs have the same unique hexagonal carbon lattice as carbon nanotubes (CNTs), confined to a quasi-one-dimensional structure. Hence, they share a variety of interesting physical characteristics. Experimental evidence of ballistic electronic transport, large phase coherence lengths, and current density sustainability,[2] accompanied by theoretical predictions and experimental verification of interesting magnetic properties,[3–9] quasirelativistic behavior,[10–13] and band gap engineering capabilities,[14–17] mark GNRs as potential building blocks in future nanoelectronic devices. Furthermore, due to their planar geometry, standard lithographic techniques may be used for the flexible design of a variety of experimental devices[1,2,10,13,17] in a controllable and reproducible manner.

Despite the aforementioned similarities, there is a distinct difference between CNTs and GNRs. Unlike the tubular shaped nanotubes, GNRs, which are long and narrow strips cut out of a two-dimensional graphene sheet, present long and reactive edges prone to localization of electronic states. The importance of these edge states was demonstrated for the case of armchair CNTs which present a metallic and nonmagnetic[18,19] character in their tubular form, but when unrolled into the corresponding zigzag GNRs, they were predicted to become semiconducting[9,20] with a spin-polarized[3–9] ground state. This ground state is characterized by opposite spin orientations of localized electronic states at the two edges of the GNR, which couple through the graphene backbone via an antiferromagnetic (AF) arrangement of spins on adjacent atomic sites.

In a recent study, Son *et al.*[9] have shown that upon the application of an electric field, an opposite local gating effect of the spin states on the two edges of the ribbon may occur. The in-plane field (perpendicular to the periodic axis of the ribbon) drives the system into a half-metallic state where one spin flavor exhibits a metallic behavior, while the opposite experiences an increase in the energy gap. Chemical doping of the ribbon edges was shown to enhance this effect resulting in an efficient and robust spin filter device.[21,22]

Following these studies on the half-metallic nature of *one-dimensional* zigzag graphene nanoribbons, several papers on the electronic properties,[23] magnetic properties,[24–27] and the half-metallic nature[28,29] of *quasi-zero-dimensional* graphene-based structures have appeared. These concluded that the spin-polarized character of the zigzag graphene edges persists also in nanometer scale islands of graphene and that the half-metallic nature of the structures studied by Son *et al.*[9] may be an artifact of the level of theory they applied.[28]

It is the purpose of our paper to present a comprehensive and systematic analysis of the electronic properties of finite-sized graphene nanoribbons. We present a general rule of thumb for the existence of a spin-polarized ground state in aromatic carbon based materials and identify the molecules $C_{28}H_{14}$ (phenanthro[1,10,9,8-opqra]perylene) and $C_{36}H_{16}$ (tetrabenzo[bc,ef,kl,no]coronene) as the smallest hydrocarbon structures to possess a magnetic ground state. The stability of the magnetic ordering, the energy gap dependence on the dimensions of the system, and the effect of an externally applied electric field are also studied. Unlike previous studies,[28] we show that the half-metallic nature of the ribbons (whether periodic or finite) is robust and insensitive to the level of theory used.

II. METHOD

To this end, we study a large set of finite rectangular nanoribbons of different widths and lengths using three levels of density functional approximations. We notate the ribbons according to the number of hydrogen atoms passivating the edges, such that an $N \times M$ finite ribbon has N hydrogen atoms on its armchair edge and M atoms on its zigzag edge (see Fig. 1). The ribbons we consider constitute three subsets corresponding to three ribbon widths: $4 \times M$, $6 \times M$, and 8

 ©2008 The American Physical Society

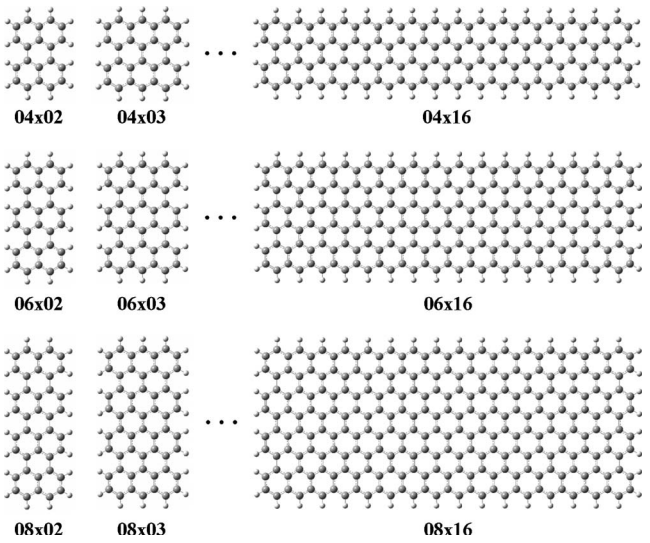

FIG. 1. The three sets of finite GNRs studied. The notation corresponds to the number of hydrogen atom passivating the edges. An $N \times M$ ribbon has N hydrogens on the armchair edge and M hydrogens on the zigzag edge.

$\times M$, where $M=2,\ldots,16$. All the calculations presented in this work were carried out using the development version of the GAUSSIAN suite of programs.[30] Spin-polarized ground state calculations were performed using the local spin density approximation,[31] the semilocal gradient corrected functional of Perdew, Burke, and Ernzerhof[31–33] (PBE), and the screened exchange hybrid density functional due to Heyd, Scuseria, and Ernzerhof (HSE06),[31,34–36] which has been tested in a wide variety of materials and has been shown to accurately reproduce experimental band gaps[37,38] and first and second optical excitation energies in metallic and semiconducting single walled CNTs.[39,40] The inclusion of short-range exact exchange in the HSE06 functional makes it suitable to treat electronic localization effects[41–45] which are known to be important in this type of materials.[3–9,16,20,21,46–54] This is further supported by the good agreement which was recently obtained between predicted band gaps[15] of narrow nanoribbons and measured values.[17] To obtain a reliable ordering of the different magnetization states, we find it important to relax the geometry of the finite GNRs for each spin polarization. Therefore, unless otherwise stated, all reported electronic properties are given for fully optimized structures for each approximate functional using the polarized 6-31G** Gaussian basis set.[55] It should be noted that since our calculations are performed within a single determinantal framework, we can determine only the total spin vector projection along a given axis m_s and not the total spin.

III. RESULTS AND DISCUSSION

Given that most organic molecules are known to be diamagnetic, while periodic[3–9,21] and finite graphene clusters[24–26,28] are predicted to have a spin-polarized ground state, we begin by studying the emergence of magnetic ordering in ultrashort and ultranarrow rectangular graphene nanoribbons. In Figs. 2(a)–2(e), we present the ground state spin density of representative structures of each of the subsets studied as obtained using the HSE06 density functional. All the structures studied have compensated lattices in the sense that the number of carbon atoms belonging to each graphene sublattice is balanced. Therefore, according to Lieb's theorem for bipartite lattices,[26,56] they have no total spin moment. The two smallest structures that present magnetic ordering in their ground state are found to be the phenanthro[1,10,9,8-opqra]perylene (bisanthrene) isomer of the $C_{28}H_{14}$ molecule and the tetrabenzo[bc,ef,kl,no]coronene isomer of the $C_{36}H_{16}$ molecule. The latter was recently identified as spin polarized using gradient corrected and hybrid density functionals.[27] This is a remarkable finding regarding the expected aromatic hydrocarbon nature of these two isomers especially in light of a previous study that predicted the ground state to be diamagnetic and the first excited state to be of diradical nature [see Fig. 2(f)].[57] Hence, our HSE06 results suggest that the energy gain from the antiferromagnetic ordering of spins obtained in the hexaradical Clar structure [see Fig. 2(g)] is higher than the aromatic stabilization even for this small organic molecule.

From a qualitative analysis of the spin density maps, we conclude that the edge atoms can be divided into three subgroups: atoms which distinctly belong to a zigzag edge, atoms that distinctly belong to an armchair edge, and atoms belonging to the seam region between the two types of edges [see Fig. 2(d)]. As a rule of thumb, we find that for rectangular ribbons of width $N=4$ and above, every carbon atom that distinctly belongs to a zigzag edge will be spin polarized. Seam region edge atoms will have a lower spin polarization, while edge atoms on a pure armchair edge are considerably less polarized. Therefore, the $N \times 2$ structures, which have no distinct zigzag edge atoms, present a diamagnetic ground state, while the $N \times 3$ (and longer) structures have magnetic ordering in their ground state.

An interesting finding is the fact that the maximum Mulliken spin polarization on the zigzag edge carbon atoms seems to be approximately constant for all the systems studied and depends mostly on the density functional chosen. For the local density approximation, this value is usually between 0.26 and 0.30, whereas the maximum Mulliken spin density is within 0.30–0.37 at the PBE level of theory. For the HSE functional, the range is 0.40–0.47. A second important conclusion is that for the short systems ($3 \lesssim M \lesssim 8$), the energetic ordering of the spin states is $E_{\uparrow\downarrow} < E_{\uparrow\uparrow} < E_0$. Here, $E_{\uparrow\downarrow}$ is the total energy of the antiferromagnetic ground state (Fig. 2), $E_{\uparrow\uparrow}$ is the energy of the ferromagnetic arrangement with a total spin moment projection of $m_s=1$ and parallel spins on both zigzag edges [see Fig. 3(a)], and E_0 is the total energy of the diamagnetic state. For longer ribbons, while the ground state remains antiferromagnetic, the above lying state is not necessarily the $m_s=1$ state anymore. The number of unpaired electrons is not sufficient to sustain the desired maximum spin polarization on the zigzag edges while maintaining the ferromagnetic ordering. Instead, a mixed configuration is obtained where both spin polarizations appear on the same ribbon edge forming a type of a short spin wave [Fig. 3(b)]. As a result, the energy of the $m_s=1$ state is raised,

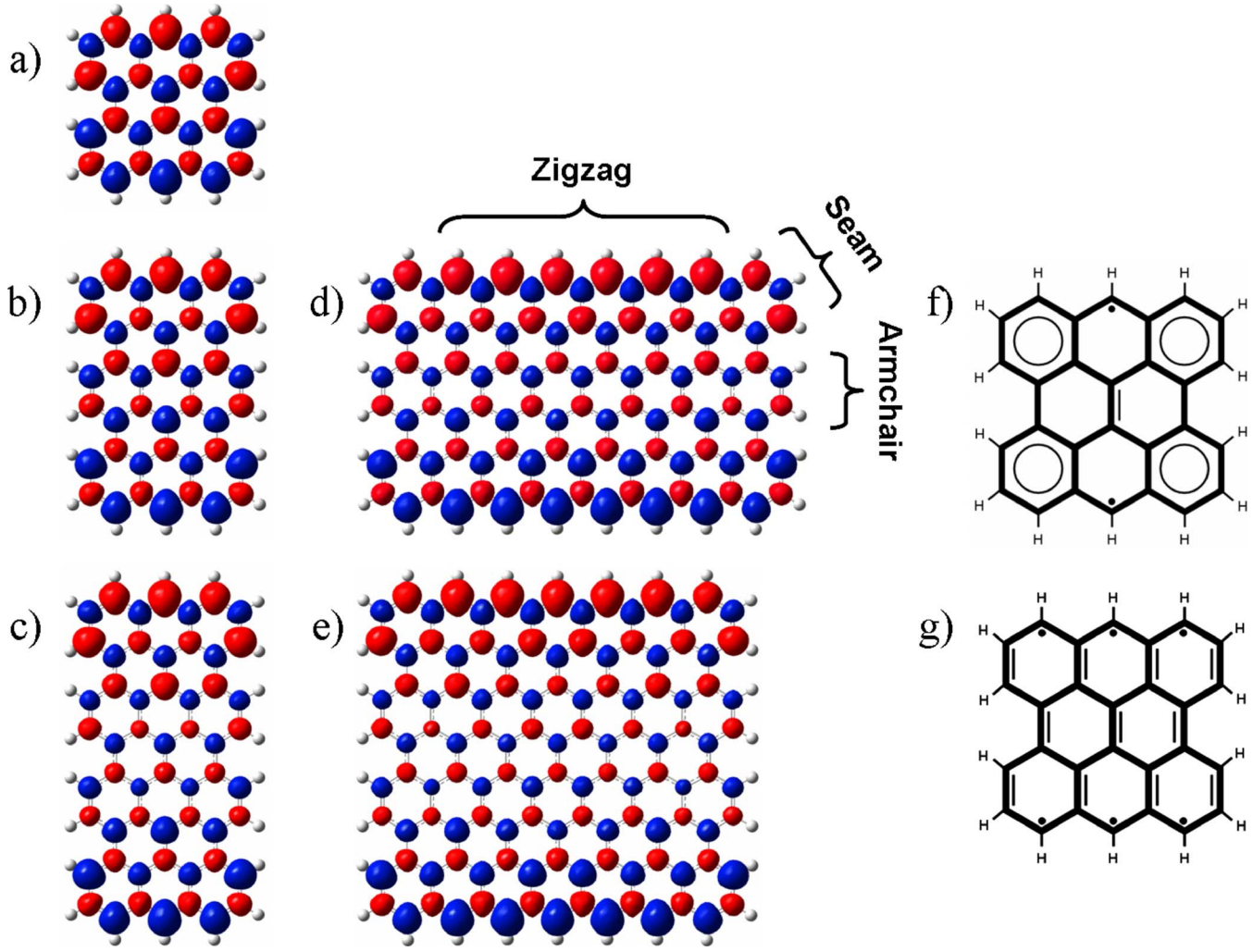

FIG. 2. (Color online) Isosurface spin densities of the antiferromagnetic ground state of the (a) 04×03, (b) 06×03, (c) 08×03, (d) 06×08, and (e) 08×07 GNRs as obtained using the HSE06 functional and the 6-31G** basis set. The sorting of the atoms into zigzag, armchair, and seam regions is indicated in (d). (f) and (g) represent the diradical and hexaradical Clar structures of bisanthrene.

usually above the $m_s=2$ state, which in turn becomes the lowest energy state with finite total spin.

To quantify these findings, we study the stability of the antiferromagnetically ordered ground state with respect to the above lying higher spin multiplicity state. In Fig. 4, the energy differences between the antiferromagnetic ground state and the first higher spin multiplicity state are presented for the three sets of ribbons studied. All diagrams are characterized by sharp maximum structures that correspond to the ribbon length at which a transition in the magnetization nature of the first higher spin state occurs, as discussed above. We note that even though the antiferromagnetic state of 04×03 (bisanthrene), as calculated at the HSE06 level of theory, is only 0.003 eV (30 K) below the above lying ferromagnetic state, the 04×04 structure has an energy difference of ~0.15 eV (1700 K), suggesting the detectability of its magnetic ordering even at room temperature. Furthermore, the HSE06 results indicate considerably large energy differences between the antiferromagnetic ground state and higher spin states for all ribbons with $N\geqslant4$ and length exceeding 1 nm.

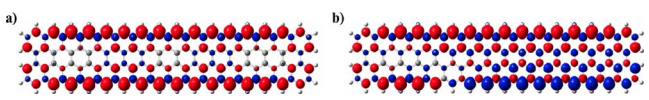

FIG. 3. (Color online) Spin density isosurfaces of the 04×16 GNR high spin multiplicity states as obtained at the PBE/6-31G** level of theory. (a) Ferromagnetic arrangement of the $m_s=3$ state. (b) Mixed configuration of the $m_s=1$ state presenting a short spin wave on one of the zigzag edges.

Before discussing the effect of an electric field on the electronic properties of finite nanoribbons, it is essential to study their ground state characteristics in the absence of external perturbations. The geometry dependence of the highest occupied molecular orbital and lowest unoccupied molecular orbitals (HOMO-LUMO) gap would be the most important parameter to address. In Fig. 5, the energy gap as a function of the length of the ribbon are presented, for the three subsets of ribbons considered and the three density functional approximations used. Even though up to now we have regarded the studied structures as zigzag nanoribbons, one can also

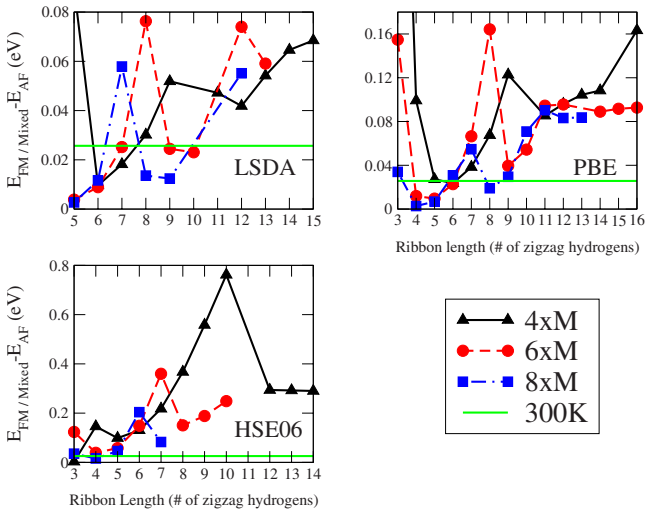

FIG. 4. (Color online) Energy differences between the antiferromagnetic (AF) ground state and the above lying higher spin multiplicity ferromagnetic (FM) or mixed state for the three sets of ribbons studied, as calculated by the local spin density approximation (upper left panel), PBE functional (upper right panel), and the HSE06 functional (lower left panel). The horizontal line represents k_BT at room temperature. Notice the different energy scales obtained for the different functional calculations.

think of them as wide and short armchair ribbons due to their finite length. These types of ribbons are known to present remarkable band-gap oscillations as a function of the ribbon width[14,15] for infinitely long armchair GNRs. Such oscillations can be clearly seen in Fig. 5 especially for the PBE results (upper right panel). The periodicity of the oscillation appears to be somewhat different than the threefold period obtained for the infinitely long counterparts. This, however, is a result of the fact that in order to prevent dangling carbon

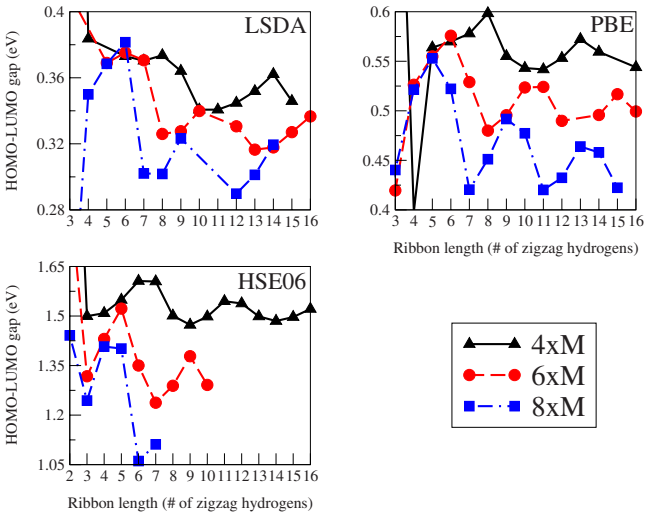

FIG. 5. (Color online) HOMO-LUMO gap values for the three sets of ribbons studied, as calculated by the local spin density approximation (upper left panel), PBE functional (upper right panel), and the HSE06 functional (lower left panel). Notice the different energy scales obtained for the different functional calculations.

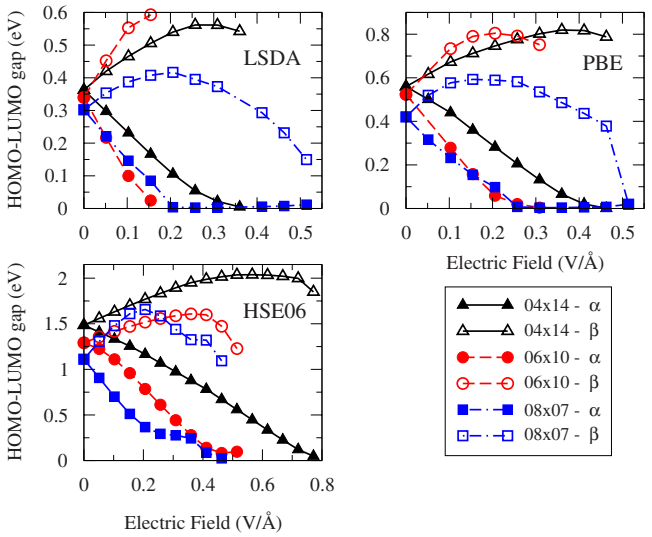

FIG. 6. (Color online) Spin-polarized HOMO-LUMO gap dependence on the strength of an external in-plane electric field for three representative finite nanoribbons, as calculated by the local spin density approximation (upper left panel), PBE functional (upper right panel), and the HSE06 functional (lower left panel). Fixed geometries of the relaxed structures in the absence of the external field at each level of theory were used. Notice the different energy scales obtained for the different functional calculations.

bonds, the width step taken for the finite systems is twice that taken in the infinitely long armchair ribbon calculations. The amplitude of the oscillations is found to be considerably damped due to the finite size of the ribbons in agreement with a previous study.[24] As expected, when the length of the armchair edge (N) is increased, the oscillation amplitude increases as well. It is interesting to note that, in general, the HOMO-LUMO gap is inversely proportional to the width (N) and the length (M) of the finite GNR in accordance with the semimetallic graphene sheet limit. Therefore, in order to obtain energy gap tailoring capability, one will have to consider GNRs with long armchair edges (large N values) and short zigzag edges (small M values). This will increase the amplitude of the energy gap oscillations while maintaining overall higher gap values.

Having explored the electronic properties of unperturbed finite GNRs, we now turn to discuss the answer to the main question addressed in this study, namely, will finite nanoribbons turn half-metallic under the influence of an external electric field? In a previous study, it was argued that the inclusion of Hartree-Fock exchange in the approximate density functional, results in the disappearance of the half-metallic state.[28] This was shown to be not true in periodic systems where screened exchange (and unpublished full exact exchange) calculations have shown half-metallic behavior similar to that obtained with semilocal and gradient corrected functionals.[21] In Fig. 6, we present the spin-polarized HOMO-LUMO gap dependence on an external in-plane electric field applied perpendicular to the zigzag edge, for three representative finite GNRs. Similar to previous calculations for periodic systems,[9,21] in the absence of an external field, the α and β gaps are degenerate. Upon the application

of the field, electrons having one spin flavor experience a smooth increase in the HOMO-LUMO gap, while the opposite spin flavor experiences a decrease in the gap. This gap splitting continues up to a point where the decreased gap vanishes, creating a degenerate zero energy state. As expected, wider systems require a lower onset field to obtain this half-metallic state.[9] At this point, due to the increased mobility of the metallic electrons, further increase in the external field results in spin transfer between both edges, thus reducing the total spin polarization and the energy gap splitting. At higher electric fields, the systems become diamagnetic.[21,29] All three representative structures present the same features described above. The main difference between the LSDA, PBE, and HSE06 results is the zero-field HOMO-LUMO gap and thus the onset electric field required to induce half-metallic behavior. Nevertheless, they all predict the appearance of the half-metallic state at an appropriate electric field strength.

IV. CONCLUSIONS

To summarize, we have presented a detailed study of the electronic properties of finite rectangular graphene nanoribbons. Bisanthrene is predicted to be the smallest organic hydrocarbon structure to present a spin-polarized ground state. This state is characterized with antiferromagnetic ordering of spins at the zigzag edges of the molecule. As a rule of thumb, we find that zigzag edges that are at least three consecutive units long will present spin polarization if the width of the system is 1 nm or wider. For systems with zigzag edges 1 nm and longer, our HSE06 results predict the antiferromagnetic ordering to be considerably stable with respect to higher spin multiplicity states, suggesting the room temperature detectability of their spin polarization. Depending on the dimensions of the system, higher spin states can have antiferromagnetic ordering or be of mixed nature with spin wave characteristics. Similar to periodic ribbons, HOMO-LUMO gap oscillations with the length of the zigzag edge are observed. The amplitude of these oscillations, however, is lower than that predicted for infinite ribbons. The half-metallic nature of the ribbons under an external in-plane electric field is preserved even for finite and extremely short GNRs, regardless of the level of theory used.

ACKNOWLEDGMENTS

This work was supported by NSF Award No. CHE-0457030 and the Welch Foundation. Calculations were performed in part on the Rice Terascale Cluster funded by NSF under Grant No. EIA-0216467, Intel, and HP. O.H. would like to thank the generous financial support of the Rothschild and Fulbright Foundations.

[1] K. S. Novoselov, A. K. Geim, S. V. Morozov, D. Jiang, Y. Zhang, S. V. Dubonos, I. V. Grigorieva, and A. A. Firsov, Science **306**, 666 (2004).
[2] C. Berger, Z. Song, X. Li, X. Wu, N. Brown, C. Naud, D. Mayou, T. Li, J. Hass, A. N. Marchenkov, E. H. Conrad, P. N. First, and W. A. de Heer, Science **312**, 1191 (2006).
[3] M. Fujita, K. Wakabayashi, K. Nakada, and K. Kusakabe, J. Phys. Soc. Jpn. **65**, 1920 (1996).
[4] K. Wakabayashi, M. Sigrist, and M. Fujita, J. Phys. Soc. Jpn. **67**, 2089 (1998).
[5] K. Wakabayashi, M. Fujita, H. Ajiki, and M. Sigrist, Phys. Rev. B **59**, 8271 (1999).
[6] K. Kusakabe and M. Maruyama, Phys. Rev. B **67**, 092406 (2003).
[7] A. Yamashiro, Y. Shimoi, K. Harigaya, and K. Wakabayashi, Phys. Rev. B **68**, 193410 (2003).
[8] H. Lee, Y.-W. Son, N. Park, S. Han, and J. Yu, Phys. Rev. B **72**, 174431 (2005).
[9] Y.-W. Son, M. L. Cohen, and S. G. Louie, Nature (London) **444**, 347 (2006).
[10] Y. Zhang, Y.-W. Tan, H. L. Stormer, and P. Kim, Nature (London) **438**, 201 (2005).
[11] N. M. R. Peres, A. H. Castro Neto, and F. Guinea, Phys. Rev. B **73**, 195411 (2006).
[12] N. M. R. Peres, A. H. Castro Neto, and F. Guinea, Phys. Rev. B **73**, 241403(R) (2006).
[13] K. S. Novoselov, Z. Jiang, Y. Zhang, S. V. Morozov, H. L. Stormer, U. Zeitler, J. C. Maan, G. S. Boebinger, P. Kim, and A. K. Geim, Science **315**, 1379 (2007).
[14] M. Ezawa, Phys. Rev. B **73**, 045432 (2006).
[15] V. Barone, O. Hod, and G. E. Scuseria, Nano Lett. **6**, 2748 (2006).
[16] Y.-W. Son, M. L. Cohen, and S. G. Louie, Phys. Rev. Lett. **97**, 216803 (2006).
[17] M. Y. Han, B. Özyilmaz, Y. Zhang, and P. Kim, Phys. Rev. Lett. **98**, 206805 (2007).
[18] R. Saito, G. Dresselhaus, and M. S. Dresselhaus, *Physical Properties of Carbon Nanotubes* (Imperial College Press, London, 1998).
[19] M. S. Dresselhaus, G. Dresselhaus, and P. Avouris, *Topics in Applied Physics* (Springer, Heidelberg, 2001), Vol. 80.
[20] K. Nakada, M. Igami, and M. Fujita, J. Phys. Soc. Jpn. **67**, 2388 (1998).
[21] O. Hod, V. Barone, J. E. Peralta, and G. E. Scuseria, Nano Lett. **7**, 2295 (2007).
[22] D. Gunlycke, J. Li, J. W. Mintmire, and C. T. White, Appl. Phys. Lett. **91**, 112108 (2007).
[23] P. G. Silvestrov and K. B. Efetov, Phys. Rev. Lett. **98**, 016802 (2007).
[24] P. Shemella, Y. Zhang, M. Mailman, P. M. Ajayan, and S. K. Nayak, Appl. Phys. Lett. **91**, 042101 (2007).
[25] M. Ezawa, arXiv:0707.0349v1 (unpublished).
[26] J. Fernandez-Rossier and J. J. Palacios, Phys. Rev. Lett. **99**, 177204 (2007).
[27] D. en Jiang, B. G. Sumpter, and S. Dai, J. Chem. Phys. **127**, 124703 (2007).
[28] E. Rudberg, P. Salek, and Y. Luo, Nano Lett. **7**, 2211 (2007).

[29] Er-Jun Kan, Zhenyu Li, Jinlong Yang, and J. G. Hou, arXiv:0708.1213v1, Appl. Phys. Lett. (to be published).
[30] M. J. Frisch, G. W. Trucks, H. B. Schlegel, G. E. Scuseria, M. A. Robb, J. R. Cheeseman, J. A. Montgomery, Jr., T. Vreven, K. N. Kudin, J. C. Burant, J. M. Millam, S. S. Iyengar, J. Tomasi, V. Barone, B. Mennucci, M. Cossi, G. Scalmani, N. Rega, G. A. Petersson, H. Nakatsuji, M. Hada, M. Ehara, K. Toyota, R. Fukuda, J. Hasegawa, M. Ishida, T. Nakajima, Y. Honda, O. Kitao, H. Nakai, M. Klene, X. Li, J. E. Knox, H. P. Hratchian, J. B. Cross, C. Adamo, J. Jaramillo, R. Gomperts, R. E. Stratmann, O. Yazyev, A. J. Austin, R. Cammi, C. Pomelli, J. W. Ochterski, P. Y. Ayala, K. Morokuma, G. A. Voth, P. Salvador, J. J. Dannenberg, V. G. Zakrzewski, S. Dapprich, A. D. Daniels, M. C. Strain, O. Farkas, D. K. Malick, A. D. Rabuck, K. Raghavachari, J. B. Foresman, J. V. Ortiz, Q. Cui, A. G. Baboul, S. Clifford, J. Cioslowski, B. B. Stefanov, G. Liu, A. Liashenko, P. Piskorz, I. Komaromi, R. L. Martin, D. J. Fox, T. Keith, M. A. Al-Laham, C. Y. Peng, A. Nanayakkara, M. Challacombe, P. M. W. Gill, B. Johnson, W. Chen, M. W. Wong, C. Gonzalez, and J. A. Pople, GAUSSIAN Development Version, Revision E.05, Gaussian, Inc., Wallingford, CT, 2004.
[31] The local density, gradient corrected, and screened hybrid approximations are obtained using the SVWN5, PBEPBE, and HSE1PBE keywords in GAUSSIAN, respectively.
[32] J. P. Perdew, K. Burke, and M. Ernzerhof, Phys. Rev. Lett. **77**, 3865 (1996).
[33] J. P. Perdew, K. Burke, and M. Ernzerhof, Phys. Rev. Lett. **78**, 1396 (1997).
[34] J. Heyd, G. E. Scuseria, and M. Ernzerhof, J. Chem. Phys. **118**, 8207 (2003).
[35] J. Heyd, G. E. Scuseria, and M. Ernzerhof, J. Chem. Phys. **124**, 219906 (2006).
[36] A. F. Izmaylov, G. E. Scuseria, and M. J. Frisch, J. Chem. Phys. **125**, 104103 (2006).
[37] J. Heyd and G. E. Scuseria, J. Chem. Phys. **121**, 1187 (2004).
[38] J. Heyd, J. E. Peralta, and G. E. Scuseria, J. Chem. Phys. **123**, 174101 (2005).
[39] V. Barone, J. E. Peralta, M. Wert, J. Heyd, and G. E. Scuseria, Nano Lett. **5**, 1621 (2005).
[40] V. Barone, J. E. Peralta, and G. E. Scuseria, Nano Lett. **5**, 1830 (2005).
[41] K. N. Kudin, G. E. Scuseria, and R. L. Martin, Phys. Rev. Lett. **89**, 266402 (2002).
[42] I. D. Prodan, J. A. Sordo, K. N. Kudin, G. E. Scuseria, and R. L. Martin, J. Chem. Phys. **123**, 014703 (2005).
[43] I. D. Prodan, G. E. Scuseria, and R. L. Martin, Phys. Rev. B **73**, 045104 (2006).
[44] P. J. Hay, R. L. Martin, J. Uddin, and G. E. Scuseria, J. Chem. Phys. **125**, 034712 (2006).
[45] D. Kasinathan, J. Kunes, K. Koepernik, C. V. Diaconu, R. L. Martin, I. D. Prodan, G. E. Scuseria, N. Spaldin, L. Petit, T. C. Schulthess, and W. E. Pickett, Phys. Rev. B **74**, 195110 (2006).
[46] K. Kobayashi, Phys. Rev. B **48**, 1757 (1993).
[47] K. Nakada, M. Fujita, G. Dresselhaus, and M. S. Dresselhaus, Phys. Rev. B **54**, 17954 (1996).
[48] Y. Miyamoto, K. Nakada, and M. Fujita, Phys. Rev. B **59**, 9858 (1999).
[49] T. Kawai, Y. Miyamoto, O. Sugino, and Y. Koga, Phys. Rev. B **62**, R16349 (2000).
[50] S. Okada and A. Oshiyama, Phys. Rev. Lett. **87**, 146803 (2001).
[51] Y. Niimi, T. Matsui, H. Kambara, K. Tagami, M. Tsukada, and H. Fukuyama, Appl. Surf. Sci. **241**, 43 (2005).
[52] Y. Kobayashi, K. I. Fukui, T. Enoki, K. Kusakabe, and Y. Kaburagi, Phys. Rev. B **71**, 193406 (2005).
[53] Y. Niimi, T. Matsui, H. Kambara, K. Tagami, M. Tsukada, and H. Fukuyama, Phys. Rev. B **73**, 085421 (2006).
[54] Y. Kobayashi, K. I. Fukui, T. Enoki, and K. Kusakabe, Phys. Rev. B **73**, 125415 (2006).
[55] P. C. Hariharan and J. A. Pople, Theor. Chim. Acta **28**, 213 (1973).
[56] E. H. Lieb, Phys. Rev. Lett. **62**, 1201 (1989).
[57] J. R. Dias, J. Chem. Inf. Model. **46**, 788 (2006).